CONTAMINANT - MICROBIAL SIDEROPHORE COMPLEXES: THEIR STRUCTURE AND ENERGETICS IN SURFACE DECONTAMINATION PROCESSES

C. C. Ainsworth - Pacific Northwest National Laboratory; B. P. Hay - Pacific Northwest National Laboratory; S. J. Traina - Ohio State University; S. C. B. Myneni - Princeton University

Background

A major need associated with the DOE D&D effort is improvement of metal surface decontamination. The DOE is responsible for and disposal of approximately 180,000 metric tons of metal associated with their nuclear facilities. Continued deposition of corrosion products on the steel surfaces allows radioactive materials to be continually sorbed to secondary oxide layers, incorporated into their structure or occluded by overgrowth.

There are a wide variety of biosynthesized organic chelates termed siderophores that are specifically designed to chelate Fe under iron deficient conditions. These chelates appear to be more effective at oxide dissolution and actinide (IV) complexation than EDTA or other organic acids currently used in decontamination processes.

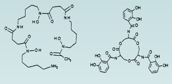

Desferrioxamine B Enterobactin

These siderophores bind hard acids [Fe(III) and actinides(IV)] with extraordinarily high affinities. For example, the binding constant for the siderophore enterobactin with Fe is about 10^{50} and its binding constant for Pu(IV) is estimated to be as high if not higher.

LFER relationships depicted below for a series of oxygen donor ligands (Lewis Bases) shows that siderophores with catecholate functional groups have the potential to bind strong lewis acids; e.g., Fe^{3+} and the tetravalent actinides. Similar results are predicted for the hydroxamate functional group siderophores.

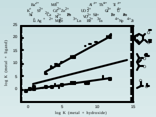

Linear free energy relationships (LFR) for catechol, acetylacetonate, and acetate for a series of metals.

Project Goals

The project is investigating the efficacy of using siderophores (or siderophore like chelates) as decontamination agents. The specific goals of this project are:

- To develop an improved understanding of the interaction between siderophores (and their functional moieties), Fe and actinide oxides, their surface chemical pro perties that foster their dissolution, and the conditions that maximize that dissolution.
- To develop the computational tools necessary to predict the rea ctivity of different siderophore functional groups toward oxide dissolution and actinides solubilization.
- To identify likely candidate chelates for use in decontamination processes.

The overall research products will be 1) fundamental knowledge relating the surface chemistry and properties of oxide/contaminant interactions and their dissolution/sequestration by these organic chelates, and 2) development of the information necessary to tailor siderophore structure and properties to EM's disparate metal surface decontamination needs.

Task Structure and Content

Research is being performed within four tasks. These tasks are focused on central investigative themes (i.e., macroscopic dissolution studies, optical spectroscopy, XAS, and computational chemistry).

Task 1. Macroscopic Dissolution Studies - PNNL, OSU
- Determine the dissolution rates of oxides common to steel corrosion products as a function of pH ligand concentration and ligand type.
- Determine the effect of sorbed contaminants on oxide dissolution and solubilization of contaminants.

Task 2. Optical Spectroscopy - PNNL
- Identify dominant surface species responsible for oxide dissolution.

Task 3. X-ray Absorption Spectroscopy - OSU, Princeton
- Identify the structure and coordination chemistry of Cr substituted Fe oxides and sorbed contaminants.
- Their interactions (structure & coordination) with siderophoretype ligands.

Task 4. Computational Chemistry - PNNL
- Extend the MM3 model parameter set to treat catechol- and hydroxamate-type ligands and their Fe and f-block metal complexes.
- Correlate ligand structure/reactivity with dissolution rates.

Experimental Materials

Oxides

Hematite (α -Fe_2O_3), Maghemite (γ -Fe_2O_3), and Cr substituted series produced in quantity for use in these studies. Other selected oxides, goethite (α -FeOOH) and Uraninite (UO_2), are being used in specific cases.

Theoretical Solid	Average Formula of Solid	Surface Area (m^2/g)
[a]Hematite Series		
Fe_2O_3	Fe_2O_3	40
$Fe_{1.90}Cr_{0.10}O_3$	$Fe_{1.97}Cr_{0.03}O_3$	69
$Fe_{1.80}Cr_{0.20}O_3$	$Fe_{1.93}Cr_{0.07}O_3$	106
$Fe_{1.50}Cr_{0.50}$	$Fe_{1.69}Cr_{0.01}O_3$	55
$FeCrO_3$	----	----
$Fe_{0.5}Cr_{1.5}O_3$	------	----
Cr_2O_3	Cr_2O_3	10
[a]Maghemite Series		
Fe_2O_3	Fe_2O_3	22
$Fe_{1.80}Cr_{0.20}O_3$	$Fe_{1.88}Cr_{0.12}O_3$	40
$Fe_{1.50}Cr_{0.50}O_3$	$Fe_{1.82}Cr_{0.18}O_3$	51
Goethite	FeOOH	53

[a] D. G. Beak, C-C. Chen, J. M.Bighamand S. J.Traina 1999. Synthesis and Properties of Hematite/Maghemite and Their Chromium Substituted Analogs. Presented at the 1999 Clay Minerals Society Meetings.

Siderophores

For the over 200 siderophores isolated, almost all are ligands containing hydroxamic acid, aminocarboxylates and/or catechol groups; deferriferrioxamine B is a common hydroxamate siderophore and enterobactin is a catacholate siderophore.

Currently, studies are utilizing three commercial hydroxamates:
- Deferriferrioxamine B -trihydroxamate
- Rhodotorulic acid - dihydroxamate
- Actohydroxamic acid - monohydroxamate

Catecholate and aminocarboxylate siderophores are being cultured. Siderophoreanalogs to be utilized are:

Catecholates
- agrobactin: *Agrobacterium tumefaciens* (ATCC 23308)
- Bis-catecholate (being synthesized)
- Catechol

Aminocarboxylates
- rhizoferrin: *Rhizopus microsporus* var. *rhizopodiformis* (ATCC 66276)
- Gylcine

Selected Results From Fe Oxide Dissolution Studies

Oxide Dissolution Studies - Methods

- pH-stat batch system under N_2 atmosphere
- ~4g/L oxide suspension; 0.1 M $NaNO_3$ background electrolyte
- ligand concentration proportional to number of functional groups (i.e., [aHA] = 0.01 M; [RTA] = 0.005 M; [DEF] = 0.0033 M
- 3-mL suspension samples removed periodically (over 48 h), filtered, and analyzed by atomic absorption spectroscopy
- 1st-order rate constants determined for log-linear data (>20 h)

Selected Properties and Structure of Hydroxamic Acid Ligands Used in These Studies.

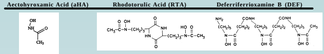

	Aectohyroxamic Acid (aHA)	Rhodotorulic Acid (RTA)	Deferriferrioxamine B (DEF)
log K_H (H_xL = $H_{x-1}L$ + H)	(1) 9.36	(1) 9.44 (2) 8.49	(2) 9.70 (3) 9.03 (4) 8.39
logβ (Fe,L,H)	21.09 (1,2,0) 28.29 (1,3,0)	21.55 (1,1,0) 62.2 (2,3,0) (logβ$_{230}$ per Fe^{+3} =31.1)	30.5 (1,1,1)

Geothite dissolution by the three hydroxamic acids at pH values ranging from 4.5 to 9.0 are shown below.
- In all cases, dissolution exhibits two components - an initial rapid rate (indicative of highly reactive sites) followed by a slower 1st-order rate.
- Clearly, aHA does not promote dissolution to the extent of the RTA or DEF, despite the greater initial ligand concentration.
- aHA promoted oxide dissolution exhibits substantial pH dependence
- RTA and DEF exhibit only limited pH dependence with respect to total [Fe] solubilized after 48 h or the 1st-order rate constant (estimated 1st order rate constants are listed below).

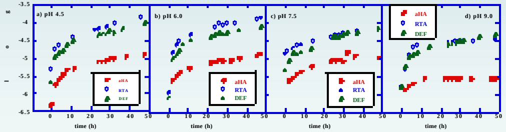

Estimated 1st-order rate constants for Goethite Dissolution by aHA, RTA and DEF

pH	aHA	RTA	DEF
	h^{-1} ($x10^3$)		
4.5	8.5	8.0	15.1
6.0	7.9	9.6	10.9
7.5	3.4	7.2	11.7
9.0	-	3.7	10.1

For simple organic ligands, the ligand-promoted rate of oxide dissolution is directly proportional to the surface sorbed ligand concentration[1-5], if:
- The reaction is far from equilibrium;
- Surface structure and stoichiometry don't change greatly with pH;
- Surface coordination is between a single ligand and surface metal atom;
- The water-promoted rate is small compared to proton- and ligand-promoted dissolution rates; and
- All adsorption sites contribute to dissolution in a similar manner.

Under these conditions the rate law is expressed as:

$$R = k_L [\Gamma L]^l + k_p [\Gamma H^+]^p$$

where the k's are rate constants for ligand-(L) and proton-(P) promoted dissolution, the superscripts are the respective rate orders and Γ L and Γ H^+ are the surface concentrations for ligands and protons.

While it has been assumed that the above conditions necessary for the rate law expression are valid for the present goethite studies, the data below suggests that aHA (at the higher pH values) may not be far enough from equilibrium The $[Fe]_{aq}$ generated by RTA (data not shown) and DEF ligand-promoted dissolution of goethite are well below the calculated equilibrium concentrations for all pH values studied. Horizontal lines represent calculated $[Fe]_{aq}$ at pH 4.5 and 7.5 in equilibrium with the appropriate ligand concentration and excess goethite.

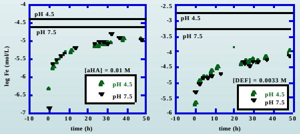

Based on preliminary estimates, the ligand surface densities do not appear to be substantially different (see table below).

Approximate Surface Densities of aHA, RTA and DEF on Goethite[a]

pH	aHA	RTA	DEF
	mol/m^2 ($x10^7$)		
4.5	2.5	3.8	4.0
6.0	2.4	3.9	3.9
7.5	2.2	3.2	4.2
9.0	1.6	2.8	4.0

[a]preliminary data from 10-min batch sorption studies at [L] used in dissolution studies; data is difficult to obtain and highly variable.

Conclusions:

- The initial rapid flux of $[Fe]_{aq}$ is probably due to dissolution of high energy surface sites rather than self-poisoning via FeL complex readsorption.
- Hematite dissolution studies (data not shown) exhibit similar behavior as goethite for aHA, but RTA and DEF exhibit even less pH dependence.
- Based on solubility calculations, hematite ligand-promoted dissolution exceeds Fe solubility limits by almost 4 orders of magnitude; this is probably due to the formation of a hydrous surface layer that is more akin to ferrihydrite than hematite.
- Considering the difference in $[L]_{aq}$ and initial estimates of [Γ L], it is unclear at this time if ligand adsorption densities ca n explain the substantially greater dissolution exhibited by RTA and DEF.
- Because of the flexibility of the hydroxamate functional groups associated with RTA and DEF, the surface structure of RTA and DEF during the dissolution rate - determining step (detactment) may differ from that of aHA; thereby increasing the slow step rate.

Quantitative Structure-Function Relationships via Molecular Modeling

Approach

Model Development:

The MM3 program is one of the best molecular mechanics models for simple organic molecules. Additional parameters must be developed to allow application of MM3 to specific ligands and to their metal complexes. Our first task was to adapt the MM3 model to treat one class of complexes, Fe(III) catecholamides. This was accomplished by:
- Adding parameters for catecholamide ligands
- Adding parameters for Fe(III) + catecholamide complexes
- Model validation by comparison to known structures and energeti cs

Experimental structure-function data for the set of structurally varied tris- catecholamides depicted below are available in the form of pFe values measured in aqueous solution at 10 mM ligand, 1 mM Fe(III), and pH 7.4.

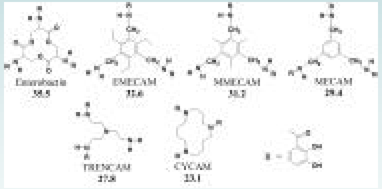

Model Application:

The modified MM3 model yielded a structure-function relationship for Fe(III) complexation by a series of tris- catecholamide architectures. This was accomplished by:
- Conformational searches to identify the lowest energy Fe(III) complex structures
- Conformational searches to identify the lowest energy ligand structures
- Correlating calculated energy differences with experimental binding affinities.

Model Development: Adding parameters for catecholamide ligands

The default MM3 force field is missing parameters for several key interactions that determine the conformation of the ligands examined in this study. Two examples are shown to the right. Missing parameters were derived by fitting to geometries and energies from electronic structure calculations. For rotational potential surfaces, single point energies at optimized B3LYP geometries were done at the MP2/DZP level. For hydrogen bonds, single point energies were done at the MP2/aug-cc-pVTZ level.

Additional torsional parameters were required to reproduce the rotational potential surface for the amide-arene bond. The plot shows the MM3 parameter fit to the MP2/DZP calculation results.

Additional hydrogen bonding parameters were required to treat the interaction between a phenol hydroxyl donor and an amide oxygen acceptor. These were fit to MP2/aug-cc-pVTZ geometries and interaction energies.

Model Development: Adding parameters for Fe(III)catecholamide complexes

The MM3 force field was extended to treat Fe(III)-catecholamide complexes using a Points-on-a-Sphere model. This was done using a minimal set of Fe(III)-dependent interactions: Fe -O stretch, Fe O-C bend, and Fe- O-C- C torsion. Parameter development entailed fitting to crystal structure data, and fitting to geometries and potential energy surfaces for an [Fe(III)(catecholate)$_3$]$^{3-}$ model complex calculated with density functional theory at the VWN/DZVP2/A2 level.

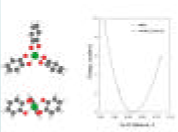

Two views of the structure of the [Fe(III)(catecholate)$_3$]$^{3-}$ complex and the MM3 parameter fit to the symmetric Fe- O stretching potential obtained at the VWN/DZVP2/A2 level of theory.

Model Development: Validation

The performance of the extended MM3 model was checked by the ability to reproduce experimental structures and known barriers for octahedral inversion.

Overlays and rmsd values for calculated versus X- ray structures. For metals other than Fe(III), we used the same parameter set except that the M- O distance was constrained to the average X-ray value with a large force constant.

Model Application: Conformational searches on Fe(III) complexes.

The most stable geometries for the six tris -catecholamide Fe(III) complexes are depicted above.

Model Application: Conformational searches on the ligands.

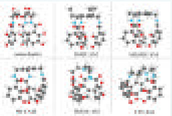

The most stable geometries for the six protonated tris catecholamide ligands

Model Application: Correlation of structure with binding affinity

Analysis of the results led to the first quantitative structureactivity relationship for catechol-amide ligands. After conformational searches to identify the lowest energy structures, we obtained the difference in steric energy between the Fe(III) complex and the metal-free protonated ligand. This energy difference correlates with the observed Fe(III) binding affinity. This result suggests that this method can be used to screen other candidate architectures for ligands based on the catechol-amide group.

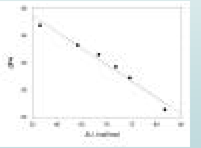

A plot showing the correlation between pFe and ΔU (calculated difference in steric energy between the Fe(III) complex and the protonated ligand, both in their lowest energy conformations.

Future Studies

Task 1. Dissolution studies
- Catecholate dissolution of Fe oxides
- Siderophore dissolution of UO_2
- Siderophore dissolution of Cr substituted Fe oxides
- Influence of surface contaminants on oxide dissolution

Task 2. Continue FT-IR studies to identify hydroxamate and catecholate surface structures on Fe oxides and UO_2.

Task 3. X-ray absorption spectroscopy
- Metal contaminant speciation at the surface of Fe and Fe/Cr Oxides.
- Interaction of simple siderophore functional group analogs at the surfaces of oxides.

Task 4. Computational chemistry
- Adapt the MM3 model to treat the Fe(III) hydroxamate siderophores.
- Adapt the MM3 model to treat the Fe(III) aminocarboxylate siderophores.

EMSP/D&D Impacts

Contaminants associated with steel surface films, corrosion pits, and cracks are present as mixed solids or surface sorbed species. Regardless of where they reside, the critical step in decontamination is the dissolution of the oxide surface film. Siderophores are suspected to be more effective at oxide dissolution and actinide complexation than EDTA or other synthetic chelates currently used in decontamination processes.

Research conducted on this project is motivated by field and laboratory observations concerning the importance of metal oxides and their associated contaminants in biogeochemistry as applied to decontamination of steel and is directed at:

- Exploring the fundamental scientific aspects of oxide mineral surface chemistry related to ligand-promoted dissolution and associated contaminant solubilization;
- Targeting how, under what conditions, and which types of siderophore-like compounds are best suited for decontamination of metal surfaces; and
- Developing the capability to identify specific siderophore like chelates best suited for decontamination and the conditions for optimal efficiency.

Literature Cited

1. Holmen, B. A. and W. H. Casey. (1996) Hydroxamate ligands, surface chemistry, and the mechanism of ligand-promoted dissolution of goethite [α -FeOOH(s)]. *Geochim. Cosmochim. Acta* 60, 4403-4416.

2. Furrer, G. and W. Stumm (1986) The coordination chemistry of weathering: I. Dissolution kinetics of δ-Al_2O_3 and BeO. *Geochim. Cosmochim. Acta*, 50, 1847-1860.

3. Stumm, W. and R. Wollast (1990) Coordination chemistry of weathering: Kinetics of the surface controlled dissolution of oxide minerals. *Rev. Geophysics*, 28, 53-69.

4. Zinder, B., G. Furrer and W. Stumm (1986) The coordination chemistry of weathering. II. Dissolution of Fe(III) oxides. *Geochim. Cosmochim. Acta*, 50, 1861-1869.

5. Amrhiem, C. and D. L. Suarez (1988) The use of a surface complexation model to describe the kinetics of ligand-promoted dissolution of anorthite. *Geochim.Cosmochim. Acta*, 52, 2785-2793.

Office of Science and Office of Environmental Management
Environmental Management Sciences Program